Proposal for a Ramsey Neutron-Beam Experiment to Search for Ultralight Axion Dark Matter at the European Spallation Source

P. Fierlinger
School of Natural Sciences, Technical University Munich, 85748 Garching, Germany

M. Holl
European Spallation Source ERIC, 224 84 Lund, Sweden

D. Milstead
Physics Department, Stockholm University, 106 91 Stockholm, Sweden

V. Santoro
Faculty of Science, Department of Physics, Lund University, 221 00 Lund, Sweden and European Spallation Source ERIC, 224 84 Lund, Sweden

W. M. Snow
Department of Physics, Indiana University, Bloomington, Indiana 47405, USA

Y. V. Stadnik
School of Physics, The University of Sydney, Sydney, New South Wales 2006, Australia

(Received 4 May 2024; accepted 23 September 2024; published 29 October 2024)

High-intensity neutron beams, such as those available at the European Spallation Source (ESS), provide new opportunities for fundamental discoveries. Here, we discuss a novel Ramsey neutron-beam experiment to search for ultralight axion dark matter through its coupling to neutron spins, which would cause the neutron spins to rotate about the velocity of the neutrons relative to the dark matter halo. We estimate that experiments at the HIBEAM beamline with a 50 m free flight path at the ESS can improve the sensitivity to the axion-neutron coupling compared to the current best laboratory limits by up to 2–3 orders of magnitude over the axion mass range 10^{-22} eV–10^{-16} eV.

DOI: 10.1103/PhysRevLett.133.181001

Introduction—Astrophysical and cosmological observations indicate that about one-quarter of the total energy and five-sixths of the total matter content of the Universe is due to dark matter (DM) [1], the identity and microscopic properties of which remain a mystery. Traditional detection schemes have largely focused on searching for possible particlelike signatures of weakly interacting massive particles (WIMPs) with masses in the ∼GeV–TeV range [2], whose signatures scale to the fourth power of a small interaction constant between the DM and ordinary matter. On the other hand, ultralight bosons with sub-eV masses and a high particle number density may produce distinctive wavelike signatures. One of the leading candidates for DM is the axion, which is a light pseudoscalar (spin-0, parity-odd) particle originally proposed to resolve the strong $\mathcal{CP}$ problem of quantum chromodynamics (QCD) [3–9]. Besides the canonical QCD axion, more generic axionlike particles (ALPs) may also exist in nature [10,11]. (In the following, we do not distinguish between the canonical QCD axion and axionlike particles and simply refer to both as "axions.") ALPs may arise as pseudo-Nambu-Goldstone bosons of a broken global symmetry or from string and field theoretical models at intermediate, GUT or Planck scales. The masses of ALPs are expected to be generated via nonperturbative effects and thus suppressed exponentially relative to some fundamental scale, which readily allows ALPs with masses much lighter than the μeV-to-meV "classical" axion mass window. Direct searches for axion DM have thus far mainly focused on the axion's possible electromagnetic coupling to photons [12].

Neutron-beam experiments have been employed for many types of fundamental physics tests, such as neutron-antineutron oscillations, electric dipole moment searches, new-boson-mediated forces, and investigations of the structure of the weak interaction; see, e.g., Refs. [13–24]. Intense

Published by the American Physical Society under the terms of the Creative Commons Attribution 4.0 International license. Further distribution of this work must maintain attribution to the author(s) and the published article's title, journal citation, and DOI. Funded by SCOAP^3.

slow neutron beams available at neutron sources enable high precision measurements and searches in fundamental physics [25–27]. Presently under construction, the European Spallation Source (ESS) [28] will open a new window at the so-called intensity frontier. In particular, the ESS has a capability for a long magnetically controlled beamline [23] and provides a unique sensitivity increase for a range of phenomena using the ESS's high-flux pulsed source. Here, we discuss a specific example of an experiment that can leverage the new capabilities of such sources to explore new physics. We evaluate the sensitivity of a Ramsey experiment at such a pulsed neutron beam facility to a pseudomagnetic field effect stemming from the coupling of an ultralight axion DM field to the neutron. The derivative coupling of axion DM to neutron spins would cause neutron spins to precess about the velocity of the neutrons relative to the DM halo. Depending on the orientation of the pseudomagnetic field with respect to the experiment, this would cause neutrons in the beam to accumulate an additional phase as they travel along their flight path. We estimate that with the proposed HIBEAM neutron beamline [23] at the ESS, the sensitivity to the axion-neutron coupling can be improved compared to the current best laboratory limits by up to 2–3 orders of magnitude over the axion mass range 10^{-22} eV–10^{-16} eV.

The intense, pulsed slow neutrons in the beam of our proposed setup, combined with the long flight path and stringent magnetic field control, would be unique in the world and enable new types of fundamental physics neutron beam experiments. For example, the addition of polarized neutron birefringent optical devices [29,30] to HIBEAM as outfitted for our proposed ALP search would enable sensitive investigations of *CPT* and Lorentz-invariance violation in neutron spin-gravitational couplings [31,32], experimental tests of macrorealistic theories using Leggett-Garg inequalities for neutrons [33–35], and a measurement of the neutron Sagnac effect [36–38] in the quantum limit using mode entangled neutron beams [39]. Neutron beamlines longer than HIBEAM are routinely used in pulsed spallation neutron source scattering experiments for practical applications.

Theory—Ultra-low-mass axions with very small kinetic energies can be produced efficiently via nonthermal production mechanisms, such as vacuum misalignment [40–42] shortly after the big bang, and can subsequently form a coherently oscillating classical field: $a(t) \approx a_0 \cos(\omega t)$, with the angular frequency of oscillation given by $\omega \approx m_a c^2/\hbar$, where m_a is the axion mass, $\hbar$ is the reduced Planck constant, and c is the speed of light in vacuum. The oscillating axion field carries the energy density $\rho_a \approx m_a^2 a_0^2/2$ and behaves like a cold, nearly pressureless fluid on length scales greater than the de Broglie wavelength of the field. (Unless indicated otherwise, we adopt the natural units $\hbar = c = 1$ in this Letter.) Cosmological and astrophysical observations rule out the possibility of axions with masses $m_a \lesssim 10^{-21}$ eV comprising the dominant fraction of the DM [43–46], although such ultralight axions may still comprise a subdominant fraction of the DM depending on their mass. Gravitational interactions between axion DM and ordinary matter during galactic structure formation subsequently virialize galactic axions ($v_{\rm vir} \sim 300$ km/s locally), which gives an oscillating axion field in our local Galactic region the finite coherence time: $\tau_{\rm coh} \sim 2\pi/(m_a v_{\rm vir}^2) \sim 2\pi \times 10^6/m_a$; i.e., $\Delta\omega/\omega \sim 10^{-6}$ corresponding to nearly monochromatic oscillations of the field.

An axion field may interact with nucleons via the derivative coupling:

$$\mathcal{L}_{\rm int} = -\frac{C_N}{2f_a}\partial_\mu a \bar{N}\gamma^\mu\gamma^5 N, \qquad (1)$$

where N and $\bar{N}$ denote the nucleon field and its Dirac adjoint, respectively, f_a is the axion decay constant, and C_N is a model-dependent dimensionless parameter. The spatial components of the derivative coupling of an oscillating axion DM field in the laboratory frame of reference, $a(t, \boldsymbol{r}) \approx a_0 \cos(m_a t - \boldsymbol{p}_a \cdot \boldsymbol{r})$, with spin-polarized nucleons in Eq. (1) simplifies as follows in the nonrelativistic limit [47,48]:

$$H_{\rm int}(t) \approx \frac{C_N a_0}{2f_a}\sin(m_a t)\boldsymbol{\sigma}_N \cdot \boldsymbol{p}_a \equiv \boldsymbol{\sigma}_N \cdot \boldsymbol{B}_{\rm eff}(t), \qquad (2)$$

which resembles the interaction of a nucleon spin $\boldsymbol{\sigma}_N$ (which has unity norm, $|\boldsymbol{\sigma}_N| = 1$) with a time-varying *pseudomagnetic* field $\boldsymbol{B}_{\rm eff}(t)$. The interaction in Eq. (2) causes nucleon spins to precess about the direction of the axion DM momentum $\boldsymbol{p}_a$, taken in the laboratory frame. The correlation $\boldsymbol{\sigma}_N \cdot \boldsymbol{p}_a$ in Eq. (2) is modulated at the daily sidereal frequency due to the rotation of Earth and can be calculated by transforming to a nonrotating celestial coordinate system; see, e.g., [49–51] for more details. The average value of $\boldsymbol{p}_a$, sampled over many coherence times, is expected to be directed opposite to the laboratory's orbital motion about the Galactic Center. However, due to the stochastic nature of the axion DM field [52], the magnitude and direction of $\boldsymbol{p}_a$ during the course of measurements may differ from the long-term average value [53,54].

The "axion wind" spin-precession effect described by Eq. (2) induces temporal variations in the Larmor precession frequency of a polarized nucleon spin according to

$$\hbar\omega_L(t) = |-\gamma_N \boldsymbol{\sigma}_N \cdot \boldsymbol{B} + 2\boldsymbol{\sigma}_N \cdot \boldsymbol{B}_{\rm eff}(t)|, \qquad (3)$$

principally from the component of $\boldsymbol{B}_{\rm eff}(t)$ directed along the applied magnetic field $\boldsymbol{B}$, with γ_N being the gyromagnetic ratio of the nucleon. A (pseudo) magnetic-field measurement using a neutron spin is based on measurement of the phase $\phi(T) = \int_0^T \omega_L(t)dt$, where T is the spin precession time, resulting in a measurement sensitivity that depends not only on the coupling constant C_n/f_a, but also on the axion mass: for the most sensitive scenario in an experiment when $m_a \ll \omega_L$, in which case $\boldsymbol{B}_{\rm eff}$ is approximately constant during the free precession phase and a phase can continuously build up. Note that the axion-DM-induced change in the Larmor precession frequency scales linearly in the small interaction constant, in contrast to the quadratic scaling in searches for virtual-axion-mediated spin-dependent forces [55].

Experimental apparatus—To measure a change in ω_L, Ramsey's method of separated oscillating fields [56] is used. The method is based on the comparison of ω_L to an external frequency ω_1 from a stable clock. Polarized neutrons enter a spin-flipper coil, a region with a magnetic field $\boldsymbol{B}_1$, oscillating at a frequency ω_1. This closely approximates a rotating magnetic field at frequency ω_L determined by the constant background field $\boldsymbol{B}_0$. B_1 is adjusted to ultimately result in a spin rotation by $\pi/2$ radians, into the plane normal to $\boldsymbol{B}_0$, resulting in a precession at the Larmor frequency ω_L. The neutrons then precess in the constant magnetic field $\boldsymbol{B}_0$ for a time T, where a phase $\phi = \omega_L T$ is built up. At the end of the flight path, a second $\pi/2$ flip is applied by passage through a second coil, driven with the same current that also drives the first coil. In the case when $\omega_L = \omega_1$, both $\pi/2$-flips add up, resulting in a downward pointing polarization of the neutron. A mismatch of the frequencies, such that a phase π is built up during the flight time relative to ω_1, results in the polarization pointing upward. Performing many independent Ramsey experiments with different settings for ω_1 results in the well-known Ramsey fringes. An unknown magnetic-field-like effect, as well as any other magnetic field applied in addition to $\boldsymbol{B}_0$, will shift the whole pattern in frequency. Repeatedly determining the central fringe of the pattern for subsequently different $\boldsymbol{B}_0$ orientations thus reveals a slowly oscillating offset field $\boldsymbol{B}_{\rm eff}$ or its absence within the boundaries of statistical and systematic precision. This can then be converted into the parameter space of coupling constant and axion mass. A constant magnetic field $\boldsymbol{B}_0$ is obtained with magnetic shielding around the field-generating coil and neutron flight path. However, the axion DM field is not necessarily affected by the passive magnetic shield based on a ferromagnetic alloy and a (regular) conductive shield [57]. A flight time of ~50 ms for a length of 50 m with high statistics and a 10 Hz repetition rate allow for a sensitive bandwidth to an oscillating field with frequency from around 3 Hz (corresponding to an axion mass of 10^{-14} eV) to below mHz.

The experimental setup is shown in Fig. 1: it starts with a collimated beam of 10×10 cm^2 size at the entrance to the apparatus, calculated using McStas [58]. From 10^{12} neutrons per second initially [23], the number of neutrons reaching the detector becomes 2×10^{10} per pulse. The magnetic

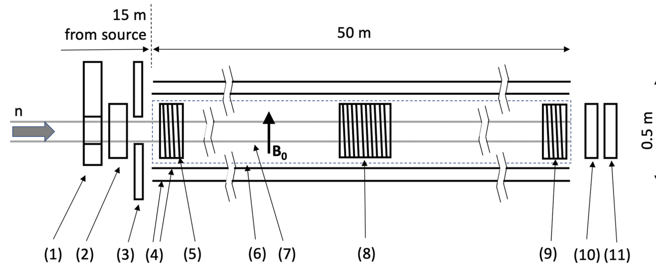

FIG. 1. Schematic setup of the experiment (longitudinal cut). Neutrons enter from the left; (1) is a chopper; (2) a polarizer; (3) a collimator. The neutrons then enter a magnetically controlled region denoted with a dashed line (6), where a magnetic field $\boldsymbol{B}_0$ is applied; the field is surrounded by a two-layer passive magnetic shield (4); (7) is the vacuum chamber with a neutron guide; (5) and (9) are the $\pi/2$ spin flippers; (8) is an optional π spin flipper; (10) is a spin analyzer; and (11) is a detector.

field can be applied in any transverse direction. The setup is situated starting 15 meters from the ESS moderator [59]. The whole length of the flight path is magnetically shielded and a constant magnetic field is applied.

Sensitivity—Statistical sensitivity: The frequency resolution of a single Ramsey experiment scales as

$$\Delta f = \frac{1}{2\pi T \alpha \sqrt{N}}, \tag{4}$$

with N being the number of neutrons and α the contrast in detection of the different spin states. The sensitivity then increases with the square root of the number of repetitions, while the oscillations of the DM field remain coherent. The initial neutron flux from the moderator into the exit of the neutron extraction system is 1×10^{12} n/s, which is subsequently reduced by polarization ($\times 0.5$), polarization analysis ($\times 0.5$), and calibration runs ($\times 0.8$). Here, we assume a quasi-perfectly fit elliptic neutron guide section with $m \sim 3$ to capture practically the whole flux. Also, the spin flippers are assumed to be perfectly efficient over the entire velocity range. Assuming only systematic errors uncorrelated with the frequency of the DM oscillation signal, the experiment is statistically limited. Of particular interest is the use of the full neutron pulse without a neutron chopper to use the full strength of the beam.

A frequency resolution of 10^{-8} rad/s can be reached in one year of run-time for a 50-meter flight path. As the signal is measured as a time-dependent modulation of the magnetic field, the effect alternatingly adds and subtracts from the magnetic field, thus effectively doubling the precision to 5×10^{-9} rad/s. Using Eq. (2), this translates into the sensitivity estimates shown in Fig. 2, assuming that axions saturate the observed density of DM in our local Galactic region, $\rho \approx 0.4$ GeV/cm^3 [1]. The sensitivity is estimated by a simulation of the so-called Ramsey fringes, which is the polarization P_z along the magnetic field $\boldsymbol{B}_0$ as a function of the detuning from the resonance frequency ω_L.

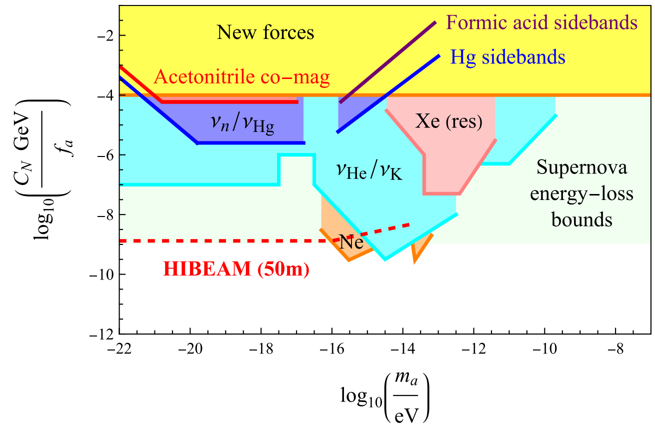

FIG. 2. Projected sensitivity of a 50 m scale Ramsey neutron-beam experiment using the HIBEAM neutron beamline at the ESS (denoted by dashed red line) to the coupling strength of axion dark matter with a neutron, defined in Eq. (1), as a function of the axion mass m_a, assuming one year of run-time and that axions saturate the observed density of dark matter in our local Galactic region, $\rho \approx 0.4\ \text{GeV/cm}^3$ [1]. The cyan, blue, orange, pink, red, and purple regions indicate regions of parameter space already probed by magnetometry-based searches for time-varying spin-precession effects induced by axion dark matter [50,60–69]. The yellow region denotes the region of parameter space ruled out by a magnetometry-based search for spin-dependent forces mediated by the exchange of virtual axions [55]. The pale green region denotes bounds from astrophysical observations of supernovae [70], which are subject to model-dependent assumptions and may be evaded altogether [71].

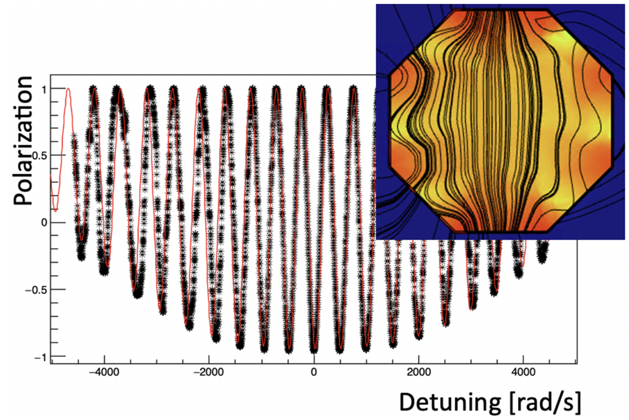

FIG. 3. Ramsey fringes for a realistic magnetic field. The inset shows a cut through the octagonal field setup with illustrated field lines.

The parameters varied in the simulation are the spread of measurements with different detuning, neutron statistics, duration of the neutron pulse, magnetic field maps, spin-flip pulses, neutron positions, momentum directions and velocities, the precession time T, the duration of a $\pi/2$-flip τ, the frequency Ω_R related to B_1 (the Rabi frequency), and the detuning $\delta\omega$ from the Larmor frequency.

Magnetic field: The phase buildup during free precession depends on the homogeneity of the magnetic field. The field is obtained by a two-layer octagonal passive magnetic shield with open ends and its axis approximately aligned with the neutron beam central axis. The shield houses a coil made from eight longitudinal wires to produce a transverse magnetic field with a relative homogeneity at the level of 10^{-3} over the volume occupied by the neutron beam (see inset in Fig. 3).

The vacuum tube, which also acts as a shield for higher frequencies, is accessed for pumping at the detector region only, as the vacuum requirement is only 10^{-5} mbar. The passive shield design is similar to that in Ref. [72].

Polarization: When the neutrons enter the shielded region, they pass through a cell containing polarized ^{3}He. Through spin-dependent nuclear absorption of neutrons on ^{3}He, an almost perfectly polarized neutron beam ($> 99\%$) can be obtained, thus hardly affecting contrast in the Ramsey measurement. Polarization analysis after the Ramsey experiment can be done in the same way. We use cells made from nondepolarizing glass [73] to obtain spin life-times of the order of a day, with polarization done using the spin-exchange optical pumping technique with a similar setup as in [74] with a length of several cm, a diameter of 0.1 m and a pressure of up to 10 bar. Cell designs are conceptually based on [75]. The product of polarization and analysis power determines the contrast parameter α in Eq. (4). Spin-flipper coils are composed of approximately 50 turns of wire wound around a nonmetallic support inside the vacuum chamber to minimize coupling to the chamber and shields; both spin-flipper coils are serially connected and fed by a function generator, stabilized by a GPS-locked frequency standard. While the $\pi/2$ condition is only perfectly valid for a single velocity, the analysis works for a range of velocities but with reduced contrast. With a B_1 amplitude of $\sim 100\ \mu\text{T}$, corresponding to 3000 spin rotations per second, and for a $\pi/2$-flip at 1200 m/s, the corresponding coil length is 0.1 m. Placed along the flight path, a π flipper is installed, which can be deployed. In particular, it can reduce washout of the phase measurement due to geometry; e.g., in the form of parity-symmetric magnetic-field deformations along the shield for a centered beam. A further interesting feature is that it can recover the flip angles for velocities that do not match the $\pi/2$-flip conditions and thus massively broaden the velocity acceptance of the Ramsey setup. However, for our new physics search, a symmetric placement in a constant field also strongly suppresses sensitivity to the new-physics signal in the most interesting frequency range and thus will only be used for instrument characterization. It should be noted that the magnitude of $\boldsymbol{B}_0$ does not change the new physics reach. However, a smaller field makes the experiment more sensitive to background gradients. The second spin flip and the polarization analysis are similar to the first spin flip and polarizer, respectively.

Pulse duration and velocity spread: The duration of a pulse at the ESS is ∼3 ms at a 10 Hz repetition rate. Although the phase information is washed out, a fit of the central fringes of the Ramsey experiment can in principle resolve the phase information. A neutron chopper can be used to refine the pulse.

Neutron detection: The detector is assumed to be a generic neutron detector that is sufficiently pixelized over an area of about $20 \times 20\ \mathrm{cm}^2$ to allow the detection of a high count rate of $\sim 10^{10}$ neutrons per second localized to temporal bins of 0.1 s. For 10 000 pixels, for example, this corresponds to a ∼10 MHz count rate. We will use a 2D-position-sensitive segmented ion chamber using ^{3}He as the absorber in the gas. Similar detectors have been successfully used in several sensitive polarized neutron transmission experiments conducted at both pulsed and continuous neutron sources to search for parity-odd neutron interactions with nuclei and for possible exotic spin-dependent neutron interactions [76–78].

Discussion and conclusions—Neutron physics offers the potential to probe new physics in ultralight axion DM searches. As shown in Fig. 2, our proposed experiment at the HIBEAM neutron beamline at the ESS has significant discovery potential, offering up to 2–3 orders of magnitude improvement in sensitivity compared to the current best laboratory limits. Using free neutrons as a probe of the "axion-wind" spin-precession effect in Eq. (2) provides a clean probe of the neutron interaction parameter C_n/f_a, which is complementary to the magnetometry approaches in Refs. [50,60–69] that involve nuclei and hence probe linear combinations of proton and neutron interaction parameters [79]. Our proposed experiment is expected to be competitive with bounds from astrophysical observations of supernovae [70], while also offering the advantage of a much cleaner and better controlled environment. The interpretation of rare astrophysical phenomena, such as supernova explosions, which take place in conditions drastically different from those in the laboratory, require additional model-dependent assumptions that may not be valid [71].

Acknowledgments—The work of Y. V. S. was supported by the Australian Research Council under the Discovery Early Career Researcher Award No. DE210101593. W. M. S. acknowledges support from the U.S. National Science Foundation (NSF) Grant No. PHY-2209481 and the Indiana University Center for Spacetime Symmetries. D. M. and V. S. gratefully acknowledge support from the Council for Swedish Research Infrastructure for the Swedish Research Council for the grant "HIBEAM pre-studies." V. S. gratefully acknowledges support from the Stiftelsen för Strategisk Forskning for the grant "Development of a magnetic control beamline for fundamental physics and condensed matter science at the European Spallation Source."

[1] Particle Data Group *et al.*, Review of particle physics, Prog. Theor. Exp. Phys. **2022**, 083C01 (2022).
[2] Leszek Roszkowski, Enrico Maria Sessolo, and Sebastian Trojanowski, WIMP dark matter candidates and searches—Current status and future prospects, Rep. Prog. Phys. **81**, 066201 (2018).
[3] R. D. Peccei and H. R. Quinn, *CP* conservation in the presence of instantons, Phys. Rev. Lett. **38**, 1440 (1977).
[4] Steven Weinberg, A new light boson?, Phys. Rev. Lett. **40**, 223 (1978).
[5] F. Wilczek, Problem of strong *P* and *T* invariance in the presence of instantons, Phys. Rev. Lett. **40**, 279 (1978).
[6] Jihn E. Kim, Weak interaction singlet and strong *CP* invariance, Phys. Rev. Lett. **43**, 103 (1979).
[7] Mikhail A. Shifman, A. I. Vainshtein, and Valentin I. Zakharov, Can confinement ensure natural *CP* invariance of strong interactions?, Nucl. Phys. **B166**, 493 (1980).
[8] Michael Dine, Willy Fischler, and Mark Srednicki, A simple solution to the strong *CP* problem with a harmless axion, Phys. Lett. **104B**, 199 (1981).
[9] A. R. Zhitnitsky, On possible suppression of the axion hadron interactions, Yad. Fiz. **31**, 497 (1980) [Sov. J. Nucl. Phys. **31**, 260 (1980)].
[10] Joerg Jaeckel and Andreas Ringwald, The low-energy frontier of particle physics, Annu. Rev. Nucl. Part. Sci. **60**, 405 (2010).
[11] Paola Arias, Davide Cadamuro, Mark Goodsell, Joerg Jaeckel, Javier Redondo, and Andreas Ringwald, WISPy cold dark matter, J. Cosmol. Astropart. Phys. 06 (2012) 013.
[12] C. B. Adams *et al.*, Axion dark matter, arXiv:2203.14923.
[13] S. Baeler, V. V. Nesvizhevsky, K. V. Protasov, and A. Y. Voronin, Constraint on the coupling of axionlike particles to matter via an ultracold neutron gravitational experiment, Phys. Rev. D **75**, 075006 (2007).
[14] V. V. Nesvizhevsky, G. Pignol, and K. V. Protasov, Neutron scattering and extra-short-range interactions, Phys. Rev. D **77**, 034020 (2008).
[15] Yu. N. Pokotilovski, Neutron experiments to search for new spin-dependent interactions, JETP Lett. **94**, 413 (2011).
[16] F. M. Piegsa and G. Pignol, A proposed search for new light bosons using a table-top neutron Ramsey apparatus, J. Phys. Conf. Ser. **340**, 012043 (2012).
[17] C. Haddock *et al.*, A search for possible long range spin dependent interactions of the neutron from exotic vector boson exchange, Phys. Lett. B **783**, 227 (2018).
[18] William Michael Snow, Chris Haddock, and Ben Heacock, Searches for exotic interactions using neutrons, Symmetry **14**, 10 (2022).
[19] E. Chanel *et al.*, The pulsed neutron beam EDM experiment, EPJ Web Conf. **219**, 02004 (2019).
[20] Ivo Schulthess *et al.*, New limit on axionlike dark matter using cold neutrons, Phys. Rev. Lett. **129**, 191801 (2022).
[21] Dirk Dubbers and Bastian Maerkisch, Precise measurements of the decay of free neutrons, Annu. Rev. Nucl. Part. Sci. **71**, 139 (2021).
[22] M. Baldo-Ceolin *et al.*, A new experimental limit on neutron-antineutron oscillations, Z. Phys. C **63**, 409 (1994).
[23] V. Santoro *et al.*, The HIBEAM program: Search for neutron oscillations at the ESS, arXiv:2311.08326.

[24] H. Yan and W. M. Snow, New limit on possible long-range parity-odd interactions of the neutron from neutron-spin rotation in liquid 4He, Phys. Rev. Lett. **110**, 082003 (2013).
[25] *Proceedings, International Workshop on Particle Physics at Neutron Sources 2018 (PPNS 2018): Grenoble, France, 2018*, edited by T. Jenke *et al.* (2019), https://www.epj-conferences.org/articles/epjconf/abs/2019/24/contents/contents.html.
[26] R. Alarcon *et al.*, Fundamental neutron physics: A white paper on progress and prospects in the U.S., arXiv:2308.09059.
[27] V. Santoro *et al.*, HighNESS conceptual design report: Volume II. The NNBAR experiment., J. Neutron Res. **25**, 315 (2024).
[28] S. Peggs, ESS Technical Design Report (2013), https://europeanspallationsource.se/sites/default/files/downloads/2017/09/TDR_online_ver_all.pdf.
[29] F. Li, S. R. Parnell, W. A. Hamilton, B. B. Maranville, T. Wang, R. Semerad, D. V. Baxter, J. T. Cremer, and R. Pynn, Superconducting magnetic Wollaston prism for neutron spin encoding, Rev. Sci. Instrum. **85**, 053303 (2014).
[30] S. Lu, A. A. M. Irfan, J. Shen, S. J. Kuhn, W. M. Snow, D. V. Baxter, R. Pynn, and G. Ortiz, An operator analysis of contextuality witness measurements for multimode-entangled single neutron interferometry, Phys. Rev. A **101**, 042318 (2020).
[31] Yuri Bonder, Lorentz violation in a uniform Newtonian gravitational field, Phys. Rev. D **88**, 105011 (2013).
[32] V. Alan Kosteleck and Zonghao Li, Gauge field theories with Lorentz-violating operators of arbitrary dimension, Phys. Rev. D **99**, 056016 (2019).
[33] A. J. Leggett and Anupam Garg, Quantum mechanics versus macroscopic realism: Is the flux there when nobody looks?, Phys. Rev. Lett. **54**, 857 (1985).
[34] Elisabeth Kreuzgruber, Richard Wagner, Niels Geerits, Hartmut Lemmel, and Stephan Sponar, Violation of a Leggett-Garg inequality using ideal negative measurements in neutron interferometry, Phys. Rev. Lett. **132**, 260201 (2024).
[35] S. Sponar, R. I. P. Sedmik, M. Pitschmann, H. Abele, and Y. Hasegawa, Tests of fundamental quantum mechanics and dark interactions with low-energy neutrons, Nat. Rev. Phys. **3**, 309 (2021).
[36] M. G. Sagnac, Galilean-like transformation allowed by general covariance and consistent with special relativity, Compt. Ren. **157**, 708 (1913).
[37] A. A. Michelson, H. G. Gale, and F. Pearson, The effect of the Earth's rotation on the velocity of light, II, Astrophys. J. **61**, 140 (1925).
[38] S. A. Werner, J. L. Staudenmann, and R. Collela, Effect of Earth's rotation on the quantum mechanical phase of the neutron, Phys. Rev. Lett. **42**, 1103 (1979).
[39] N. Geerits *et al.*, Measuring the angular momentum of a neutron using Earth's rotation, arXiv:2407.09307.
[40] John Preskill, Mark B. Wise, and Frank Wilczek, Cosmology of the invisible axion, Phys. Lett. **120B**, 127 (1983).
[41] L. F. Abbott and P. Sikivie, A cosmological bound on the invisible axion, Phys. Lett. **120B**, 133 (1983).
[42] Michael Dine and Willy Fischler, The not-so-harmless axion, Phys. Lett. **120B**, 137 (1983).
[43] Keir K. Rogers and Hiranya V. Peiris, Strong bound on canonical ultralight axion dark matter from the Lyman-Alpha forest, Phys. Rev. Lett. **126**, 071302 (2021).
[44] Eric Armengaud, Nathalie Palanque-Delabrouille, Christophe Yèche, David J. E. Marsh, and Julien Baur, Constraining the mass of light bosonic dark matter using SDSS Lyman-forest, Mon. Not. R. Astron. Soc. **471**, 4606 (2017).
[45] Takeshi Kobayashi, Riccardo Murgia, Andrea De Simone, Vid Iršič, and Matteo Viel, Lyman-α constraints on ultralight scalar dark matter: Implications for the early and late Universe, Phys. Rev. D **96**, 123514 (2017).
[46] Nitsan Bar, Diego Blas, Kfir Blum, and Sergey Sibiryakov, Galactic rotation curves versus ultralight dark matter: Implications of the soliton-host halo relation, Phys. Rev. D **98**, 083027 (2018).
[47] V. V. Flambaum, in *Proceedings of the 9th Patras Workshop on Axions* (WIMPs and WISPs, Mainz, Germany, 2013), http://axion-wimp2013.desy.de/e201031/index_eng.html.
[48] Y. V. Stadnik and V. V. Flambaum, Axion-induced effects in atoms, molecules, and nuclei: Parity nonconservation, anapole moments, electric dipole moments, and spin-gravity and spin-axion momentum couplings, Phys. Rev. D **89**, 043522 (2014).
[49] Yevgeny V. Stadnik, *Manifestations of Dark Matter and Variations of the Fundamental Constants in Atoms and Astrophysical Phenomena* (Springer, New York, 2017).
[50] C. Abel *et al.*, Search for axionlike dark matter through nuclear spin precession in electric and magnetic fields, Phys. Rev. X **7**, 041034 (2017).
[51] C. Smorra *et al.*, Direct limits on the interaction of antiprotons with axion-like dark matter, Nature (London) **575**, 7782 (2019).
[52] Andrei Derevianko, Detecting dark-matter waves with a network of precision-measurement tools, Phys. Rev. A **97**, 042506 (2018).
[53] Gary P. Centers *et al.*, Stochastic fluctuations of bosonic dark matter, Nat. Commun. **12**, 7321 (2021).
[54] Mariangela Lisanti, Matthew Moschella, and William Terrano, Stochastic properties of ultralight scalar field gradients, Phys. Rev. D **104**, 055037 (2021).
[55] G. Vasilakis, J. M. Brown, T. W. Kornack, and M. V. Romalis, Limits on new long range nuclear spin-dependent forces set with a K-^{3}He comagnetometer, Phys. Rev. Lett. **103**, 261801 (2009).
[56] Norman F. Ramsey, A molecular beam resonance method with separated oscillating fields, Phys. Rev. **78**, 695 (1950).
[57] D. F. Jackson Kimball, J. Dudley, Y. Li, S. Thulasi, S. Pustelny, D. Budker, and M. Zolotorev, Magnetic shielding and exotic spin-dependent interactions, Phys. Rev. D **94**, 082005 (2016).
[58] P. K. Willendrup and K. Lefmann, McStas (i): Introduction, use, and basic principles for ray-tracing simulations, J. Neutron Res., **22**, 1 (2020).
[59] L. Zanini, K. H. Andersen, K. Batkov, E. B. Klinkby, F. Mezei, T. Schönfeldt, and A. Takibayev, Design of the cold and thermal neutron moderators for the European Spallation

Source, Nucl. Instrum. Methods Phys. Res., Sect. A **925**, 33 (2019).
[60] Teng Wu *et al.*, Search for axionlike dark matter with a liquid-state nuclear spin comagnetometer, Phys. Rev. Lett. **122**, 191302 (2019).
[61] Antoine Garcon *et al.*, Constraints on bosonic dark matter from ultralow-field nuclear magnetic resonance, Sci. Adv. **5**, eaax4539 (2019).
[62] Itay M. Bloch, Yonit Hochberg, Eric Kuflik, and Tomer Volansky, Axion-like relics: New constraints from old comagnetometer data, J. High Energy Phys. 01 (2020) 167.
[63] Min Jiang, Haowen Su, Antoine Garcon, Xinhua Peng, and Dmitry Budker, Search for axion-like dark matter with spin-based amplifiers, Nat. Phys. **17**, 1402 (2021).
[64] Itay M. Bloch, Gil Ronen, Roy Shaham, Ori Katz, Tomer Volansky, and Or Katz, New constraints on axion-like dark matter using a floquet quantum detector, Sci. Adv. **8**, eabl8919 (2022).
[65] Itay M. Bloch, Roy Shaham, Yonit Hochberg, Eric Kuflik, Tomer Volansky, and Or Katz, Constraints on axion-like dark matter from a SERF comagnetometer, Nat. Commun. **14**, 5784 (2023).
[66] C. Abel *et al.*, Search for ultralight axion dark matter in a side-band analysis of a ^{199}Hg free-spin precession signal, SciPost Phys. **15**, 058 (2023).
[67] Junyi Lee, Mariangela Lisanti, William A. Terrano, and Michael Romalis, Laboratory constraints on the neutron-spin coupling of feV-scale axions, Phys. Rev. X **13**, 011050 (2023).
[68] Kai Wei *et al.*, Dark matter search with a strongly-coupled hybrid spin system, arXiv:2306.08039.
[69] Zitong Xu *et al.*, Constraining ultralight dark matter through an accelerated resonant search, Commun. Phys. **7**, 226 (2024).
[70] Pierluca Carenza, Tobias Fischer, Maurizio Giannotti, Gang Guo, Gabriel Martínez-Pinedo, and Alessandro Mirizzi, Improved axion emissivity from a supernova via nucleon-nucleon bremsstrahlung, J. Cosmol. Astropart. Phys. 10 (2019) 016.
[71] Nitsan Bar, Kfir Blum, and Guido D'Amico, Is there a supernova bound on axions?, Phys. Rev. D **101**, 123025 (2020).
[72] E. Wodey *et al.*, A scalable high-performance magnetic shield for very long baseline atom interferometry, Rev. Sci. Instrum. **91**, 035117 (2020).
[73] University of Virginia, Chemical Compositions of Various Glasses (2024), https://galileo.phys.virginia.edu/research/groups/spinphysics/glass_properties.html.
[74] N. Sachdeva *et al.*, New limit on the permanent electric dipole moment of ^{129}Xe using ^{3}He comagnetometry and SQUID detection, Phys. Rev. Lett. **123**, 143003 (2019).
[75] K. P. Coulter, A. B. McDonald, W. Happer, T. E. Chupp, and M. E. Wagshul, Neutron polarization with polarized 3-He, Nucl. Instrum. Methods Phys. Res., Sect. A **270**, 90 (1988).
[76] S. D. Penn, E. G. Adelberger, B. R. Heckel, D. M. Markoff, and H. E. Swanson, A low-noise ^{3}He ionization chamber for measuring the energy spectrum of a cold neutron beam, Nucl. Instrum. Methods Phys. Res., Sect. A **457**, 332 (2001).
[77] W. M. Snow *et al.*, A slow neutron polarimeter for the measurement of parity-odd neutron rotary power, Rev. Sci. Instrum. **86**, 055101 (2015).
[78] Ralf Lehnert, W. M. Snow, and H. Yan, A first experimental limit on in-matter torsion from neutron spin rotation in liquid ^{4}He, Phys. Lett. B **730**, 353 (2014).
[79] Y. V. Stadnik and V. V. Flambaum, Nuclear spin-dependent interactions: Searches for WIMP, axion and topological defect dark matter, and tests of fundamental symmetries, Eur. Phys. J. C **75**, 110 (2015).